Journal of Inorganic and General Chemistry
ZAAC
Zeitschrift für anorganische und allgemeine Chemie
www.zaac.wiley-vch.de
RESEARCH ARTICLE
Check for updates
DOI: 10.1002/zaac.202300178

Special Collection

NMR spectroscopic investigations on the successive implementation of nickel and zinc ions to a NacNac-dibenzofuran-Br ligand precursor

Konstantin B. Krause,[a] Beatrice Cula,[a] André Dallmann,[a] and Christian Limberg*[a]

Dedicated to Professor Rhett Kempe on occasion of his 60th birthday

The ligand precursor HNacNac-dibenzofuran-Br, **LH**, was synthesized by the condensation of 6-bromo-4-dibenzofuranamine and 4-(*N*-(mesityl)amino)pent-3-en-2-one with the aim of preparing heterodinuclear nickel/zinc complexes in two successive steps. Reacting **LH** with $Zn(HMDS)_2$, $Zn(C_6F_5)_2$ and $Zn(C_2H_5)_2$ led to the respective X-Zn-NacNac-dibenzofuran-Br complexes (X = HMDS (**2**), C_6F_5 (**3**), Et (**4**)). However, in case of **2** and **3** the subsequent treatment with $Ni(COD)_2$/TMEDA did not lead to any conversion, probably as the steric bulk imposed by the NacNac-Zn-X entities was too high. **4** did react with $Ni(COD)_2$/TMEDA, likely in the envisaged manner, but apparently the targeted product complex Et-Zn-NacNac-dibenzofuran-Ni-(TMEDA)Br, once formed, immediately reacts further via a Negishi coupling reaction, so that Br-Zn-NacNac-dibenzofuran-Et (**5**) is formed. The reaction of **4** with triethylammonium bromide led to the formation of the Br-Zn-NacNac-dibenzofuran-Br (**6**) complex that could be reacted with $Ni(COD)_2$/TMEDA successfully. All attempts to purify the product led to Zn-(NacNac-dibenzofuran-Ni(TMEDA)Br)$_2$, which is insoluble in THF and thus drives a dismutation reaction.

Introduction

Metal catalysts are often based on a mononuclear metal site with a coordinative vacancy, where a substrate can be bound, activated and converted by a reactant. For some activation processes a concerted action of two metal centers is required and in such cases it is advantageous for reactivity and selectivity, if these sites are already prearranged in the catalytically active molecule.[1–4] In heterodinuclear variants the centers may have even different properties (Lewis acidity, redox activity) that can be utilized in cooperative substrate conversion.[5–8] This principle is often exploited for natural small molecule conversion in enzymes.[9–12] However, the synthesis of heterodinuclear complexes from mononuclear precursors presents a special challenge due to possible disproportionation and selectivity problems resulting in mixtures of symmetric and asymmetric complexes. One way to steer heterodinuclearity is to utilize a ligand backbone with two different binding sites[13] (for the combination Ni/Zn, which is of relevance here see e.g.[14]). We were curious, whether a dibenzofuran unit can serve as such a backbone and allows the attachment of two different metal sites. Here we present some insights gained in a corresponding investigation using NMR spectroscopy as a diagnostic tool.

Results and Discussion

We started with 6-bromo-4-dibenzofuranamine (H_2N-DBF-Br) and envisioned the attachment of a binding pocket for one metal center, while the second one was supposed to be introduced by oxidative addition to the C–Br bond. As the binding pocket we have chosen the β-diketiminato moiety (NacNac), as this ligand has allowed for the construction of a variety of reactive metal complexes for small molecule activation[15–18] and unsymmetric variants were utilized in the past for the generation of heterobimetallic compounds.[19] As the metals we selected nickel and zinc ions; nickel, as it can be inserted into the C–Br bond starting from the oxidation state zero and subsequent redox chemistry was conceivable,[15-17,20] zinc due to its Lewis acidic properties.

The HNacNac-dibenzofuran-Br precursor, **LH**, was synthesized by the condensation of H_2N-DBF-Br and 4-(*N*-(mesityl)amino)pent-3-en-2-one using triethyloxonium tetrafluoroborate in dichloromethane (Scheme 1).[21,22] Recrystallization from methanol yielded the pure ligand precursor. From the molecular structure shown in Figure 1 an approximate distance of the two potentially bound metal centers of around 5 Å (d(Br1···H1) = 5.022 Å) can be derived.

[a] *K. B. Krause, Dr. B. Cula, Dr. A. Dallmann, Prof. Dr. C. Limberg*
Institut für Chemie
Humboldt-Universität zu Berlin
Brook-Taylor-Str. 2, 12489 Berlin, Germany
E-mail: christian.limberg@chemie.hu-berlin.de

Supporting information for this article is available on the WWW under https://doi.org/10.1002/zaac.202300178

This article is part of a Special Collection dedicated to Professor Rhett Kempe on the occasion of his 60th birthday. Please see our homepage for more articles in the collection.

Journal of Inorganic and General Chemistry
ZAAC
Zeitschrift für anorganische und allgemeine Chemie

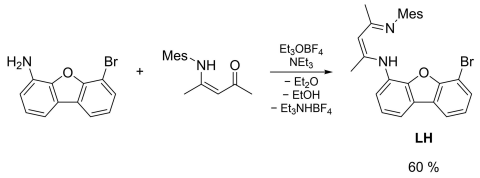

Scheme 1. Synthesis of **LH** by the reaction of H_2N-DBF-Br and 4-(*N*-(mesityl)amino)pent-3-en-2-one.

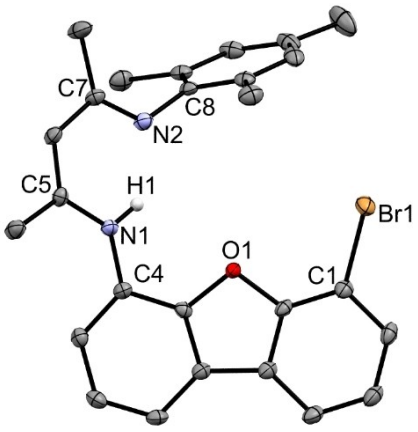

Figure 1. Molecular structure of **LH**; carbon-bound hydrogen atoms omitted for clarity; selected bond distances [Å] and angles [°]: Br1–C1 = 1.8816(16), N1–C4 = 1.4023(19), N1–C5 = 1.3651(19), N2–C7 = 1.292(2), N2–C8 = 1.4132(19), C4–N1–C5 = 129.01(13), C7–N2–C8 = 124.38(13).

Subsequently, we targeted the introduction of metal centers, starting by addressing the C–Br unit. We had shown previously that a xanthenyl iodide unit reacts with $Ni(COD)_2$ and PPh_3 to give xanthene-Ni$(PPh_3)_2$I entities.[23] To decrease the steric bulk in this case we used TMEDA (tetramethylethylendiamine) instead of phosphane co-ligands and thus reacted **LH** with $Ni(COD)_2$ in the presence of TMEDA to generate HNacNac-DBF-Ni(TMEDA)Br. This complex should feature a nickel center in a square planar coordination environment (see also below), and thus a diamagnetic behavior should be expected. However, broadened paramagnetically shifted signals appeared in the ^{1}H NMR spectrum after the reaction with $Ni(COD)_2$ (see SI, Figure S17), suggesting a different kind of coordination geometry around the nickel ion. A plausible way to rationalize this finding is to assume, that the desired complex is indeed formed initially but subsequently the organic ligand at the nickel center acts as a base for the NacNacH proton, which is transferred to the arylic position, while the nickel bromide moiety is bound in the NacNac binding pocket, leading to BrNi-NacNac-DBF-H, **1** (Scheme 2). In **1** the nickel center would have a trigonal planar coordination environment or through dimerization a tetrahedral NacNacNi(μ-Br)$_2$NiNacNac motif could form as observed for similar compounds, thus explaining the paramagnetism.[24]

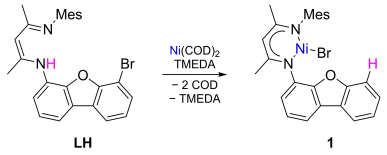

Scheme 2. Hypothetical formation of **1** upon treatment of **LH** with $Ni(COD)_2$.

Hence, in subsequent work zinc was planned to be coordinated first, ideally using precursors with basic ligands capable of deprotonating the NacNacH unit *in situ* in order to avoid a salt metathesis. $Zn(HMDS)_2$ (HMDS = hexamethlydisilazide) and $Zn(C_6F_5)_2$ were thus employed and this indeed quantitatively led to the respective X-Zn-NacNac-dibenzofuran-Br complexes (X = HMDS (**2**), C_6F_5 (**3**)), as shown by multinuclear NMR spectroscopy (Scheme 3).

However, the subsequent treatment with $Ni(COD)_2$/TMEDA did not result in any conversion of **2** or **3**, probably as the steric bulk imposed by the NacNac-ZnX entities was too high. Consequently, we used $ZnEt_2$ as the precursor next, which, as before, yielded the corresponding X-Zn-NacNac-dibenzofuran-Br complex, now with X = Et (**4**). Indeed, **4** reacted with $Ni(COD)_2$/TMEDA, likely in the envisaged manner, but apparently the targeted product complex Et-Zn-NacNac-dibenzofuran-Ni(TMEDA)Br, once formed, immediately reacts further via a Negishi coupling reaction: the ethyl and the bromide ligands at Zn and Ni are exchanged and subsequently a reductive elimination of the aryl-Et unit occurs, so that Br-Zn-NacNac-dibenzofuran-Et (**5**) forms accompanied by precipitation of elemental nickel (Scheme 4). The formation of **5** was monitored both by 1D and 2D NMR spectroscopy. While the Zn-bound ethyl group in **4** shows resonances in the ^{1}H NMR spectrum, comparable to $ZnEt_2$, at 0.94 ppm (CH_3) and 0.29 ppm (CH_2), in the course of the further reaction these signals strongly shift downfield to 1.25 ppm (CH_3) and 2.86 ppm (CH_2). These shifts

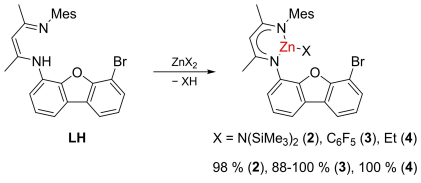

Scheme 3. Reaction of **LH** with basic zinc precursors.

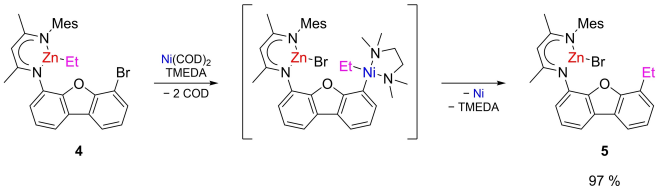

Scheme 4. Formation of **5** via a Negishi coupling mediated by $Ni(COD)_2$/TMEDA.

match an aryl-bound ethyl group well. Furthermore, the ^{1}H ^{13}C HMBC NMR spectrum confirms coupling between the ethyl group and arylic carbon atoms (see SI, Figure S19).

Consequently, now the focus shifted to X = halide to prevent side reactions upon the oxidative addition of Ni. In attempts to access X-Zn-NacNac-dibenzofuran-Br (with X = halide) via deprotonation of the ligand precursor with an appropriate base (e.g. KH) and subsequent salt metathesis with zinc halides (e.g. $ZnBr_2$) an immediate reaction was noted, leading to a mixture of products, heteroleptic as well as homoleptic complexes. Therefore, a more selective approach was pursued, and the reaction of **4** with a weak cationic Brønsted acid containing halide counter anions tested. Indeed, the application of triethylammonium bromide led to the formation of the desired Br-Zn-NacNac-dibenzofuran-Br (**6**) complex under the evolution of ethane and triethylamine as observed by NMR spectroscopy. Subsequent addition of Ni-$(COD)_2$/TMEDA resulted in a color change of the solution from the typical bright yellow exhibited by all previously discussed zinc compounds to a deep red color, and NMR spectroscopy confirmed the conversion of **6** to a new complex, presumably Br-Zn-NacNac-dibenzofuran-Ni(TMEDA)Br (**7**, Scheme 5).

However, the X-ray analysis of crystals grown from the reaction mixture by slow evaporation of the volatiles from the reaction solution revealed the structure of a trinuclear compound, **8**, featuring a homoleptic NacNac-Zn-NacNac core motif and two flanking Ni centers linked to it via the dibenzofuran backbones (Figure 2). The mesityl residues of the two ligands are parallelly aligned in a distance of 3.4 Å, with a slight displacement suggesting a π-π-stacking.[25] The zinc ion is coordinated by the four nitrogen donor atoms of the two NacNac units in a distorted tetrahedral fashion ($\tau_4 = 0.83$, $\tau_4' = 0.83$), while the coordination environment of the nickel ions is almost perfect square planar ($\tau_4 = 0.03$, $\tau_4' = 0.03$) with the planes being perpendicular to the dibenzofuran unit. Due to the insolubility of **8** in THF, it is unrealistic that the compound formed in solution upon addition of $Ni(COD)_2$/TMEDA to **6** corresponds to the compound crystallized. Rather, a dismutation of **7** into $ZnBr_2$ and **8** seems plausible, driven by the low solubility of **8** (Scheme 6).

To substantiate this hypothesis, DOSY NMR spectroscopy was utilized (see SI, Figure S20). Even though the Stokes-Einstein equation can be considered as an approximation only, the calculated values show a clear trend (Table 1). **LH** is the smallest molecule in this series and **4** and **6** show similar hydrodynamic radii. While **8** should lead to a much larger radius, the product of the reaction of **6** with $Ni(COD)_2$ shows only a slight increase in size, as one should expect for **7**. The molecular weights as determined by the ECC-method[26] exhibit the same trend and match closely the theoretical values, thus supporting the assumption of the formation of **7**.

To further support this analysis, the monometallic homoleptic complex Zn(NacNac-DBF-$Br)_2$ (**9**) was synthesized by the reaction of two equivalents **LH** with $ZnEt_2$ (Scheme 7). **9** is smaller in size than **8** but it is certainly larger than **7** and this is indeed, what is found comparing the hydrodynamic radius of **9** (r = 6.6 Å) with the one of **7** (r = 5.9 Å) as determined by DOSY NMR spectroscopy. This further supports the existence of **7** in solution, which, however cannot be crystallized due to the dismutation.

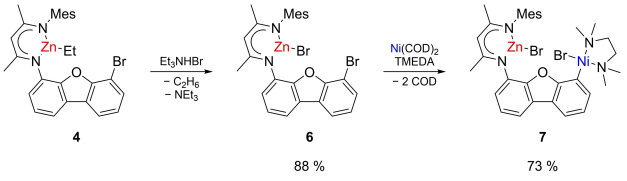

Scheme 5. Envisaged synthesis of a Zn-Ni complex.

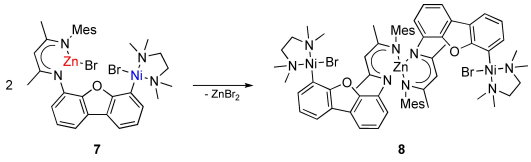

Scheme 6. Dismutation reaction of **7** into $ZnBr_2$ and **8**.

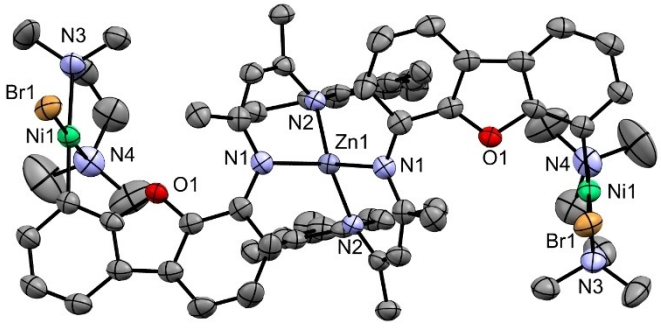

Figure 2. Molecular structure of **8**; hydrogen atoms omitted for clarity; selected bond distances [Å] and angles [°]: Zn1–N1 = 2.016(3), Zn1–N2 = 1.982(3), N1–Zn1–N2 = 94.24(12); symmetry equivalents were generated with −x, y, $^{1}/_{2}$−z.

Table 1. Diffusion coefficients according to DOSY NMR experiments in THF-d_8 ($\eta = 0.48$ mPa s^{-1}) and hydrodynamic radii after Stokes-Einstein equation as well as molecular weights as determined by the ECC-method.[26]

compound	M[a] [g mol^{-1}]	T[b] [K]	D[c] [10^{-6} cm^2 s^{-1}]	r[d] [Å]	M_{ECC}[e] [g mol^{-1}]
LH	461.40	294.1	9.810	4.6	473
4	554.84	295.6	9.143	4.9	534
6	605.68	296.0	8.513	5.3	603
7	780.58	296.0	7.617	5.9	730
9	986.17	295.6	6.857	6.6	874

[a] molecular weight. [b] temperature. [c] diffusion coefficient. [d] hydrodynamic radius. [e] molecular weight determined by the ECC-method.[26]

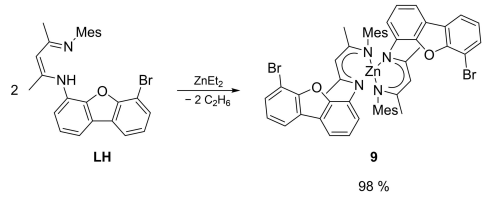

Scheme 7. Synthesis of **9** by the reaction of two equivalents of **LH** and one equivalent of $ZnEt_2$.

Conclusions

In this study we have investigated strategies to prepare heterodinuclear zinc/nickel complexes via a successive complexation/oxidative addition approach starting from a ligand precursor **LH** with a NacNac binding pocket and an aryl-Br unit. Various pitfalls were revealed. If the oxidative addition is performed first, the resulting metal ion can migrate into the NacNac site. If the NacNac site is "loaded" with a X-Zn^+ entity first, X must not be bulky, as otherwise the subsequent oxidative addition of $Ni(COD)_2$/TMEDA cannot occur. If X is a sufficiently small alkyl ligand, oxidative addition proceeds but subsequently an intramolecular Negishi coupling takes place. Hence, X has to be an inorganic ligand, which cannot be introduced via salt metathesis, though, as a simple reaction of L^- with ZnX_2 leads to homoleptic complexes. However, a bromido ligand can be introduced starting from the NacNac-Zn-Et entity, for instance, through reaction with triethyl ammonium bromide, and indeed subsequently the oxidative addition appears to proceed as planned. Attempts to isolate the product led to a unique heterotrinuclear complex, which is an insoluble component of the dismutation equilibrium. The results thus provide a useful basis for future research on heterobimetallic complexes.

Experimental Section

Materials and methods

All manipulations with air-sensitive compounds were carried out in a glovebox or by means of Schlenk-type techniques involving a dry and oxygen-free argon atmosphere. NMR spectra were recorded with Bruker DPX 300 (^{1}H 300.1 MHz), AV 500 (^{1}H 500.1 MHz, ^{13}C 125.8 MHz) and AV 600 (^{1}H 599.9 MHz) NMR spectrometers in THF-d_8, C_6D_6 and $CDCl_3$ at 25 °C if not reported differently. ^{1}H NMR spectra were calibrated against the internal residual proton and natural abundance ^{13}C resonances of the deuterated solvent. Chemical shifts (δ) were reported in ppm, coupling constants (J) in Hz. The assignment of signals was carried out with the help of 2D-analyses.

Unless stated otherwise, all starting materials were obtained from commercial sources in the highest available purity and were used without further purification. 6-Bromo-4-dibenzofuranamine was prepared according to the procedure described in literature.[27] Solvents were dried by using an MBraun Solvent Purification System SPS.

Synthetic procedures

4-(N-(mesityl)amino)pent-3-en-2-one (^{Mes}Nacac)

Acetylacetone (11.9 ml, 116 mmol, 3.0 eq.) and mesitylamine (5.44 ml, 38.6 mmol, 1 eq.) were stirred in an Anton Paar Monowave 400 microwave reactor at 210 °C for 1 h. Afterwards, the excess of acetylacetone was removed under reduced pressure. Vacuum sublimation of the brown residue at 85 °C yielded the product as a pale yellow crystalline solid (7.73 g, 35.6 mmol, 92 %).

^{1}H NMR (500.1 MHz, $CDCl_3$): δ = 11.84 (s, 1H, N*H*), 6.89 (s, 2H, $^{m-Mes}$*CH*), 5.19 (s, 1H, OC-C*H*-CNH), 2.28 (s, 3H, $^{p-Mes}$$CH_3$), 2.15 (s, 6H, $^{o-Mes}$$CH_3$), 2.10 (s, 3H, OC-C$H_3$), 1.62 (s, 3H, HN–C-C$H_3$) ppm.

^{13}C NMR (125.8 MHz, $CDCl_3$) δ = 196.0 (*C*O), 163.3 (HN-*C*-CH_3), 137.2 ($^{p-Mes}$*C*), 135.9 ($^{o-Mes}$*C*), 134.0 ($^{i-Mes}$*C*), 129.0 ($^{m-Mes}$CH), 95.8 (OC-*C*H-CNH), 29.2 (OC-*C*H_3), 21.1 ($^{p-Mes}$$CH_3$), 19.0 (HN-C-*C*$H_3$), 18.3 ($^{o-Mes}$$CH_3$) ppm.

Elemental analysis: calculated for $C_{14}H_{19}NO$: C 77.38, H 8.81, N 6.45 %; found: C 77.53, H 9.10, N 6.44 %

HNacNac-DBF-Br (LH)

A solution of triethyloxonium tetrafluoroborate (725 mg, 3.82 mmol, 1 eq.) in dichloromethane (25 ml) was added to **^{Mes}Nacac** (829 mg, 3.82 mmol, 1 eq.) dissolved in dichloromethane (50 ml) and the resulting reaction mixture was stirred for 2 h at room temperature. Subsequently, triethylamine (1 ml) was added before stirring for further 15 min. Afterwards, the reaction mixture was added to a solution of 6-bromo-4-dibenzofuranamine (1.00 g, 3.82 mmol, 1 eq.) and triethylamine (4 ml) in dichloromethane (50 ml) and stirred for 17 h. All volatiles were removed under reduced pressure and the residue was extracted with toluene to remove the oily side-product triethylammonium tetrafluoroborate. After evaporation of the toluene *in vacuo*, the crude product was dissolved in dichloromethane/hexane (1 : 1) and filtered through silica. After removal of the dichloromethane, the product was crystallized from the residual hexane and isolated as a yellow crystalline solid (1.05 g, 2.28 mmol, 60 %).

^{1}H NMR (500.1 MHz, $CDCl_3$): δ = 12.58 (s, 1H, N*H*), 7.85 (dd, J = 7.6, 1.1 Hz, 1H, $^{7-DBF}$*CH*), 7.57 (dd, J = 7.7, 1.2 Hz, 1H, $^{1-DBF}$*CH*), 7.56 (dd, J = 7.8, 1.2 Hz, 1H, $^{9-DBF}$*CH*), 7.28 (t, J = 7.7 Hz, 1H, $^{2-DBF}$*CH*), 7.18 (t, J = 7.7 Hz, 1H, $^{8-DBF}$*CH*), 7.09 (dd, J = 7.8, 1.2 Hz, 1H, $^{3-DBF}$*CH*), 6.89 (s, 2H, $^{m-Mes}$*CH*), 5.03 (s, 1H, ^{NacNac}*CH*), 2.28 (s, 3H, $^{p-Mes}$$CH_3$), 2.26 (s, 6H, $^{o-Mes}$$CH_3$), 2.10 (s, 3H, ^{NacNac}CH_3), 1.76 (s, 3H, ^{NacNac}CH_3) ppm.

^{13}C NMR (125.8 MHz, $CDCl_3$) δ = 163.7 (^{NacNac}*C*), 159.8 (^{NacNac}*C*), 153.4 ($^{6b-DBF}$*C*), 148.4 ($^{4b-DBF}$*C*), 138.8 ($^{i-Mes}$*C*), 134.9 ($^{p-Mes}$*C*), 134.1 ($^{o-Mes}$*C*), 133.9 ($^{4-DBF}$CH), 129.9 ($^{9-DBF}$CH), 128.7 ($^{m-Mes}$CH), 126.3 ($^{9b-DBF}$*C*), 125.0 ($^{1b-DBF}$*C*), 123.8 ($^{8-DBF}$CH), 123.6 ($^{2-DBF}$CH), 121.2 ($^{3-DBF}$CH), 119.8 ($^{7-DBF}$CH), 114.9 ($^{1-DBF}$CH), 104.8 ($^{6-DBF}$CBr), 96.3 (^{NacNac}CH), 21.7 (^{NacNac}CH_3), 21.0 ($^{p-Mes}$$CH_3$), 20.2 (^{NacNac}$CH_3$), 18.7 ($^{o-Mes}$$CH_3$) ppm.

Elemental analysis: calculated for $C_{26}H_{25}BrN_2O$: C 67.68, H 5.46, N 6.07 %; found: C 67.79, H 5.20, N 5.70 %

HMDS-Zn-NacNac-DBF-Br (2)

To a yellow solution of HNacNac-DBF-Br (10.0 mg, 21.7 µmol, 1 eq.) in benzene-d_6 (0.6 ml) $Zn(HMDS)_2$ (8.75 µl, 21.7 µmol, 1 eq.) was added and the resulting mixture allowed to react for 18 hours. Subsequently, NMR experiments were performed to characterize the product (98 % yield by NMR).

^{1}H NMR (500.1 MHz, C_6D_6) $\delta = 7.45$ (dd, $J = 6.5$, 2.4 Hz, 1H, $^{9-DBF}CH$), 7.43 (dd, $J = 7.7$, 1.1 Hz, 1H, $^{1-DBF}CH$), 7.33 (dd, $J = 7.9$, 1.1 Hz, 1H, $^{7-DBF}CH$), 7.15 (d, $J = 7.7$ Hz, 1H, $^{3-DBF}CH$), 7.15 (t, $J = 7.7$ Hz, 1H, $^{2-DBF}CH$), 6.83 (s, 2H, $^{m-Mes}CH$), 6.74 (t, $J = 7.8$ Hz, 1H, $^{8-DBF}CH$), 4.96 (s, 1H, $^{NacNac}CH$), 2.29 (s, 3H, $^{o-Mes}CH_3$), 2.25 (s, 3H, $^{o-Mes}CH_3$), 2.14 (s, 3H, $^{p-Mes}CH_3$), 1.83 (s, 3H, $^{NacNac}CH_3$), 1.60 (s, 3H, $^{NacNac}CH_3$), 0.04 (s, 9H, $Si(CH_3)_3$), −0.19 (s, 9H, $Si(CH_3)_3$).

^{13}C NMR (125.8 MHz, C_6D_6) $\delta = 170.0$ ($^{NacNac}C$), 168.7 ($^{NacNac}C$), 153.8 ($^{6b-DBF}C$), 150.4 ($^{4b-DBF}C$), 144.2 ($^{i-Mes}C$), 134.8 ($^{4-DBF}C$), 134.7 ($^{p-Mes}C$), 130.6 ($^{o-Mes}C$), 129.8 ($^{m-Mes}CH$), 129.6 ($^{m-Mes}CH$), 128.4 ($^{7-DBF}CH$), 126.4 ($^{9b-DBF}C$), 125.8 ($^{1b-DBF}C$), 125.5 ($^{3-DBF}CH$), 124.4 ($^{8-DBF}CH$), 124.1 ($^{2-DBF}CH$), 120.1 ($^{9-DBF}CH$), 117.8 ($^{1-DBF}CH$), 105.0 ($^{6-DBF}CBr$), 96.9 ($^{NacNac}CH$), 23.5 ($^{NacNac}CH_3$), 23.4 ($^{NacNac}CH_3$), 20.9 ($^{p-Mes}CH_3$), 19.0 ($^{o-Mes}CH_3$), 5.1 ($Si(CH_3)_3$), 4.7 ($Si(CH_3)_3$) ppm.

C_6F_5Zn-NacNac-DBF-Br (3)

To a yellow solution of HNacNac-DBF-Br (11.0 mg, 23.8 µmol, 1 eq.) in THF-d_8 or benzene-d_6 (0.6 ml) $Zn(C_6F_5)_2$ (9.5 mg, 24 µmol, 1 eq.) was added and the resulting mixture allowed to react for 1 hour. Subsequently, NMR experiments were performed to characterize the product (88 % (THF-d_8) to 100 % (benzene-d_6) yield by NMR).

^{1}H NMR (300.1 MHz, THF-d_8) $\delta = 8.01$ (dd, $J = 7.7$, 1.1 Hz, 1H, $^{9-DBF}CH$), 7.77 (dd, $J = 7.6$, 1.3 Hz, 1H, $^{1-DBF}CH$), 7.64 (dd, $J = 7.9$, 1.1 Hz, 1H, $^{7-DBF}CH$), 7.27 (t, $J = 7.8$ Hz, 2H, $^{2-DBF}CH$, $^{8-DBF}CH$), 7.17 (dd, $J = 7.8$, 1.3 Hz, 1H, $^{3-DBF}CH$), 6.78 (d, $J = 4.3$ Hz, 2H, $^{m-Mes}CH$), 5.11 (s, 1H, $^{NacNac}CH$), 2.19 (s, 3H, $^{p-Mes}CH_3$), 2.15 (s, 3H, $^{o-Mes}CH_3$), 2.07 (s, 3H, $^{o-Mes}CH_3$), 1.98 (s, 3H, $^{NacNac}CH_3$), 1.74 (s, 3H, $^{NacNac}CH_3$) ppm.

^{19}F NMR (282.4 MHz, THF-d_8) $\delta = -115.6$ (m, o-C_6F_5), −159.9 (t, J = 19.8 Hz, p-C_6F_5), −164.3 (m, m-C_6F_5) ppm.

^{1}H NMR (300.1 MHz, C_6D_6) $\delta = 7.32$-7.22 (m, 3H, $^{1-DBF}CH$, $^{3-DBF}CH$, $^{9-DBF}CH$), 7.02-6.96 (m, 2H, $^{2-DBF}CH$, $^{7-DBF}CH$), 6.75 (s, 2H, $^{m-Mes}CH$), 6.66 (t, $J = 7.8$ Hz, 1H, $^{8-DBF}CH$), 5.11 (s, 1H, $^{NacNac}CH$), 2.19 (s, 6H, $^{o-Mes}CH_3$), 2.03 (s, 3H, $^{p-Mes}CH_3$), 1.86 (s, 3H, $^{NacNac}CH_3$), 1.62 (s, 3H, $^{NacNac}CH_3$) ppm.

^{19}F NMR (282.4 MHz, C_6D_6) $\delta = -116.6$ (m, o-C_6F_5), −155.0 (t, J = 19.8 Hz, p-C_6F_5), −161.2 (m, m-C_6F_5) ppm.

EtZn-NacNac-DBF-Br (4)

To a yellow solution of HNacNac-DBF-Br (10.0 mg, 21.7 µmol, 1 eq.) in THF-d_8 or benzene-d_6 (0.6 ml) $ZnEt_2$ (2.21 µl, 21.7 µmol, 1 eq.) was added and the resulting mixture allowed to react for 4 hours. Subsequently, NMR experiments were performed to characterize the product (100 % yield by NMR).

^{1}H NMR (599.9 MHz, THF-d_8) $\delta = 7.99$ (dd, $J = 7.7$, 1.1 Hz, 1H, $^{9-DBF}CH$), 7.73 (dd, $J = 7.7$, 1.2 Hz, 1H, $^{1-DBF}CH$), 7.63 (dd, $J = 7.8$, 1.1 Hz, 1H, $^{7-DBF}CH$), 7.31 (t, $J = 7.7$ Hz, 1H, $^{2-DBF}CH$), 7.26 (t, $J = 7.8$ Hz, 1H, $^{8-DBF}CH$), 7.13 (dd, $J = 7.7$, 1.2 Hz, 1H, $^{3-DBF}CH$), 6.84 (s, 2H, $^{m-Mes}CH$), 4.97 (s, 1H, $^{NacNac}CH$), 2.23 (s, 3H, $^{p-Mes}CH_3$), 2.16 (s, 6H, $^{o-Mes}CH_3$), 1.96 (s, 3H, $^{NacNac}CH_3$), 1.69 (s, 3H, $^{NacNac}CH_3$), 0.53 (t, $J = 8.1$ Hz, 3H, CH_3), −0.38 (q, $J = 8.2$ Hz, 2H, CH_2) ppm.

^{1}H NMR (500.1 MHz, C_6D_6) $\delta = 7.40$ (dd, $J = 7.6$, 1.1 Hz, 1H, $^{9-DBF}CH$), 7.36 (dd, $J = 7.7$, 1.2 Hz, 1H, $^{1-DBF}CH$), 7.30 (dd, $J = 7.9$, 1.1 Hz, 1H, $^{7-DBF}CH$), 7.08 (t, $J = 7.7$ Hz, 1H, $^{2-DBF}CH$), 6.99 (dd, $J = 7.7$, 1.2 Hz, 1H, $^{3-DBF}CH$), 6.82 (d, $J = 0.7$ Hz, 2H, $^{m-Mes}CH$), 6.72 (t, $J = 7.8$ Hz, 1H, $^{8-DBF}CH$), 5.07 (s, 1H, $^{NacNac}CH$), 2.17 (s, 6H, $^{o-Mes}CH_3$), 2.14 (s, 3H, $^{p-Mes}CH_3$), 1.92 (s, 3H, $^{NacNac}CH_3$), 1.65 (s, 3H, $^{NacNac}CH_3$), 0.94 (t, $J = 8.1$ Hz, 3H, CH_3), 0.29 (q, $J = 8.2$ Hz, 2H, CH_2) ppm.

^{13}C NMR (125.8 MHz, C_6D_6) $\delta = 168.2$ ($^{NacNac}C$), 166.5 ($^{NacNac}C$), 153.8 ($^{6b-DBF}C$), 150.3 ($^{4b-DBF}C$), 145.4 ($^{i-Mes}C$), 136.1 ($^{4-DBF}C$), 134.0 ($^{p-Mes}C$), 130.8 ($^{o-Mes}C$), 130.4 ($^{m-Mes}CH$), 129.5 ($^{m-Mes}CH$), 128.4 ($^{7-DBF}CH$), 126.5 ($^{9b-DBF}C$), 125.5 ($^{1b-DBF}C$), 124.7 ($^{3-DBF}CH$), 124.3 ($^{8-DBF}CH$), 123.9 ($^{2-DBF}CH$), 120.0 ($^{9-DBF}CH$), 116.8 ($^{1-DBF}CH$), 105.1 ($^{6-DBF}CBr$), 97.4 ($^{NacNac}CH$), 23.3 ($^{NacNac}CH_3$), 22.5 ($^{NacNac}CH_3$), 20.9 ($^{p-Mes}CH_3$), 18.8 ($^{o-Mes}CH_3$), 12.1 (CH_3), −2.3 (CH_2) ppm.

BrZn-NacNac-DBF-Br (6)

To the reaction solution of EtZn-NacNac-DBF-Br (**4**) in THF-d_8 triethylammonium bromide (3.9 mg, 21.7 µmol, 1 eq.) was added and the resulting mixture was heated to 70 °C for 30 minutes. Subsequently, NMR experiments were performed to characterize the product (88 % yield by NMR).

^{1}H NMR (599.9 MHz, THF-d_8) $\delta = 8.01$ (dd, $J = 7.7$, 1.1 Hz, 1H, $^{9-DBF}CH$), 7.79 (dd, $J = 7.6$, 1.4 Hz, 1H, $^{1-DBF}CH$), 7.65 (dd, $J = 7.9$, 1.1 Hz, 1H, $^{7-DBF}CH$), 7.42 (dd, $J = 7.8$, 1.3 Hz, 1H, $^{3-DBF}CH$), 7.36 (t, $J = 7.7$ Hz, 1H, $^{2-DBF}CH$), 7.28 (t, $J = 7.8$ Hz, 1H, $^{8-DBF}CH$), 6.87 (s, 1H, $^{m-Mes}CH$), 6.84 (s, 1H, $^{m-Mes}CH$), 5.00 (s, 1H, $^{NacNac}CH$), 2.24 (s, 3H, $^{o-Mes}CH_3$), 2.23 (s, 3H, $^{o-Mes}CH_3$), 2.16 (s, 3H, $^{p-Mes}CH_3$), 1.94 (s, 3H, $^{NacNac}CH_3$), 1.72 (s, 3H, $^{NacNac}CH_3$) ppm.

BrZn-NacNac-DBF-Ni(TMEDA)Br (7)

To the reaction solution of BrZn-NacNac-DBF-Br (**6**) in THF-d_8 $Ni(COD)_2$ (6.0 mg, 22 µmol, 1 eq.) and TMEDA (3.6 µl, 24 µmol, 1.1 eq.) were added and the resulting yellow mixture was allowed to react for 18 hours, resulting in a color change to deep red. Subsequently, NMR experiments were performed to characterize the product (73 % yield by NMR).

^{1}H NMR (599.9 MHz, THF-d_8) $\delta = 7.61$ (d, $J = 7.5$ Hz, 1H, $^{9-DBF}CH$), 7.43 (d, $J = 7.8$ Hz, 1H, $^{3-DBF}CH$), 7.28 (d, $J = 7.6$ Hz, 1H, $^{1-DBF}CH$), 7.23 (d, $J = 7.4$ Hz, 1H, $^{7-DBF}CH$), 7.18 (t, $J = 7.7$ Hz, 1H, $^{2-DBF}CH$), 6.89 (s, 1H, $^{m-Mes}CH$), 6.86 (t, $J = 7.6$ Hz, 1H, $^{8-DBF}CH$), 6.82 (s, 1H, $^{m-Mes}CH$), 5.07 (s, 1H, $^{NacNac}CH$), 2.23 (s, 6H, $^{o-Mes}CH_3$), 2.19 (s, 3H, $^{p-Mes}CH_3$), 1.94 (s, 3H, $^{NacNac}CH_3$), 1.73 (s, 3H, $^{NacNac}CH_3$) ppm. The TMEDA ligand does not lead to distinct signals but rather to a broadened set of signals between 2.8 ppm and 1.9 ppm.[28]

Zn(NacNac-DBF-Br)$_2$ (9)

To a yellow solution of HNacNac-DBF-Br (10.0 mg, 21.7 µmol, 2 eq.) in benzene-d_6 (0.6 ml) $ZnEt_2$ (1.11 µl, 10.8 µmol, 1 eq.) was added and the resulting mixture was heated to 80 °C for 20 hours. Subsequently, NMR experiments were performed to characterize the product (98 % yield by NMR).

The ^{1}H NMR spectrum shows signal sets for different isomers. At 70 °C these signals coalesce (see SI, Figures S21 & S22).

Acknowledgements

This research was funded by the Deutsche Forschungsgemeinschaft (DFG, German Research Foundation) under Germany's Excellence Strategy – EXC 2008–390540038 – UniSysCat. Open Access funding enabled and organized by Projekt DEAL.

Conflict of Interest

The authors declare no conflict of interest.

Data Availability Statement

The data that support the findings of this study are available in the supplementary material of this article.

Keywords: Heterometallic complexes · Cooperative effects · ligand design · nickel · zinc

[1] B. Battistella, K. Ray, *Coord. Chem. Rev.* **2020**, *408*, 213176.
[2] P. Haack, C. Limberg, *Angew. Chem. Int. Ed.* **2014**, *53*, 4282–4293.
[3] A. L. Gavrilova, B. Bosnich, *Chem. Rev.* **2004**, *104*, 349–383.
[4] N. P. Mankad, *Chem. Eur. J.* **2016**, *22*, 5822–5829.
[5] W. Zhang, W. Lai, R. Cao, *Chem. Rev.* **2017**, *117*, 3717–3797.
[6] P. Lang, M. Schwalbe, *Chem. Eur. J.* **2017**, *23*, 17398–17412.
[7] H. Steinhagen, G. Helmchen, *Angew. Chem. Int. Ed.* **1996**, *35*, 2339–2342.
[8] Z. Fickenscher, E. Hey-Hawkins, *Molecules* **2023**, *28*, 4233.
[9] A. Roth, W. Plass, *Angew. Chem. Int. Ed.* **2008**, *47*, 7588–7591.
[10] J. J. Griese, V. Srinivas, M. Högbom, *J. Biol. Inorg. Chem.* **2014**, *19*, 759–774.
[11] A. Erxleben, *Front. Chem.* **2019**, *7*, DOI 10.3389/fchem.2019.00082.
[12] J. Fesseler, J.-H. Jeoung, H. Dobbek, *Angew. Chem. Int. Ed.* **2015**, *54*, 8680–8684.
[13] R. Kretschmer, *Chem. Eur. J.* **2020**, *26*, 2099–2119.
[14] A. Roth, A. Buchholz, M. Rudolph, E. Schütze, E. Kothe, W. Plass, *Chem. Eur. J.* **2008**, *14*, 1571–1583.
[15] P. Holze, B. Braun-Cula, S. Mebs, C. Limberg, *Z. Anorg. Allg. Chem.* **2018**, *644*, 973-981.
[16] P. Zimmermann, C. Limberg, *J. Am. Chem. Soc.* **2017**, *139*, 4233–4242.
[17] S. Yao, M. Driess, *Acc. Chem. Res.* **2012**, *45*, 276–287; C. E. Elwell, N. L. Gagnon, B. D. Neisen, D. Dhar, A. D. Spaeth, G. M. Yee, W. B. Tolman, *Chem. Rev.* **2017**, *117*, 2059–2107.
[18] S. M. Bhutto, P. L. Holland, *Eur. J. Inorg. Chem.* **2019**, *2019*, 1861–1869.
[19] S. Pahar, V. Sharma, B. Mahata, C. P. George, H. Sharma, K. Vanka, S. S. Sen, *Inorg. Chem.* **2022**, *61*, 17370–17377.
[20] C. Y. Lin, P. P. Power, *Chem. Soc. Rev.* **2017**, *46*, 5347–5399.
[21] D. V. Vitanova, F. Hampel, K. C. Hultzsch, *J. Organomet. Chem.* **2005**, *690*, 5182–5197.
[22] S. G. McGeachin, *Can. J. Chem.* **1968**, *46*, 1903–1912.
[23] K. Materne, C. Spröwitz, B. Braun-Cula, C. Limberg, *Z. Anorg. Allg. Chem.* **2018**, *644*, 700–705.
[24] P. Holze, B. Braun-Cula, S. Mebs, C. Limberg, *Z. Anorg. Allg. Chem.* **2018**, *644*, 973–981.
[25] C. R. Martinez, B. L. Iverson, *Chem. Sci.* **2012**, *3*, 2191–2201.
[26] R. Neufeld, D. Stalke, *Chem. Sci.* **2015**, *6*, 3354–3364.
[27] S. T. Li, B. Braun-Cula, S. Hoof, M. Dürr, I. Ivanović-Burmazović, C. Limberg, *Eur. J. Inorg. Chem.* **2016**, *2016*, 4017–4027.
[28] S. Yu, H. Wang, J. E. Sledziewski, V. N. Madhira, C. G. Takahashi, M. K. Leon, Y. B. Dudkina, Y. H. Budnikova, D. A. Vicic, *Molecules* **2014**, *19*, 13603–13613.

Manuscript received: August 16, 2023
Revised manuscript received: October 6, 2023
Accepted manuscript online: October 6, 2023

